HTML ABSTRACT + LINKS

Room-temperature ferromagnetism in well-aligned $Zn_{1-x}Co_xO$ nanorods

Jih-Jen Wu,[a] Sai-Chang Liu, and Ming-Hsun Yang
Department of Chemical Engineering, National Cheng Kung University, Tainan 701, Taiwan

(Received 19 March 2004; accepted 9 June 2004)

Diluted magnetic semiconductor $Zn_{1-x}Co_xO$ nanorods with a Curie temperature higher than 350 K have been synthesized by *in situ* doping of Co in ZnO nanorods using a simple thermal chemical vapor deposition method. Structural analyses indicated that the nanorod possesses the single-crystalline wurtzite structure and there is no segregated cluster of impurity phase appearing throughout the nanorod. The transparence of the $Zn_{1-x}Co_xO$ nanorods in the visible region has been examined by UV-visible absorption. The fundamental absorptions of the $Zn_{1-x}Co_xO$ nanorods estimated from the absorption spectra do not reveal pronounced difference from that of pure ZnO nanorods. © *2004 American Institute of Physics*. [DOI: 10.1063/1.1779958]

Diluted magnetic semiconductors (DMSs) are formed by partial replacement of the cations of the nonmagnetic semiconductors by magnetic transition-metal ions.[1] With charge and spin degrees of freedom in a single substance, DMSs have attracted considerable research efforts owing to their great potential for use as spintroinc materials.[2] Mn-doped II–VI and III–V semiconductors have been extensively studied since 1980's, however, there is still the restriction on the use of those DMSs for practical device application as a result that their Curie temperatures (T_C) are much lower than room temperature.[3] Recently, theoretical prediction of the possibility of room-temperature ferromagnetism in ZnO-based and GaN-based DMSs[4] has stimulated research interest in this field again. ZnO exhibits a hexagonal structure with a direct band gap of 3.37 eV at room temperature, which is very similar to that of GaN. Moreover, ZnO possesses a large exciton binding energy of 60 meV. The strong exciton binding energy which is much larger than that of GaN (25 meV) as well as the thermal energy at room temperature ($\sim$26 meV) can ensure an efficient exciton emission at room temperature.[5] Room-temperature UV lasing properties[6] in ZnO epitaxial films, microcrystalline thin films, nanoclusters, and nanowires have been demonstrated recently. Combining the excellent optical properties with room-temperature ferromagnetism, many practical and versatile functional spintronic devices could be made from the ZnO-based DMSs. Although rather intensive efforts on the growth of transition metal-doped ZnO films have been demonstrated using pulsed laser deposition method, their magnetic properties were not conclusive yet.[7]

The synthesis of one-dimensional (1D) single-crystalline ZnO nanostructures has been of growing interest owing to their promising application in nanoscale optoelectronic devices.[8] Recently, the formation of ZnO-related ferromagnetic 1D nanomaterials have also been reported. Yi *et al.*[9] demonstrated the fabrication of magnetic-material/semiconductor nanorods heterostructures. Ni-thickness-dependent magnetic properties due to a crossover from ferromagnetism to superparamagnetism were observed in the Ni/ZnO nanorods heterostructures. Pearton *et al.*[10] reported the catalyst-driven ZnO nanorods implanted with Mn and Co ions. Ferromagnetic properties were observed in the Mn- and Co-implanted nanorods after a high-temperature annealing. Chang *et al.*[11] demonstrated that the $Zn_{1-x}Mn_xO$ nanowires formed by an *in situ* doping method exhibit ferromagnetic behavior with T_C at 37 K. We have demonstrated a catalyst-free chemical vapor deposition (CVD) approach for the growth of the ZnO nanorods at a low temperature of around 500 °C.[12] Instead of metal/ZnO heteronanostructures or metal-ion-implanted ZnO nanorods, *in situ* synthesis of the well-aligned $Zn_{1-x}Co_xO$ nanorods using the catalyst-free CVD method is demonstrated in this work.

$Zn_{1-x}Co_xO$ nanorods were grown in a 3 in. quartz tube insert to a three-temperature-zone furnace. Zinc acetylacetonate hydrate and Co acetylacetonate ($Zn(C_5H_7O_2)_2$, Lancaster, 98% and $Co(C_5H_7O_2)_2$, Merck, >98%), which were employed to be zinc and Co sources placed on cleaned Pyrex glass containers, were loaded into the lower-temperature zones of the furnace. The temperatures were controlled to be at 130–140 °C and 135–170 °C to vaporize the Zn and Co solid reactants, respectively. The vapor was carried by a N_2/O_2 flow into the higher-temperature zone of the furnace in which substrates were located. The total pressure of the quartz tube was 200 Torr during $Zn_{1-x}Co_xO$ nanorods growth. The morphology and size distribution of the nanorods were examined using scanning electron microscopy [(SEM) JEOL, JSM-6700F)]. Elemental analyses were conducted using electron probe x-ray microanalyzer [(EPMA) JEOL, JXA-8600SX)]. The crystal structure of the nanorods was analyzed using x-ray diffraction [(XRD) Rigaku D/MAX-2000] and high-resolution transmission electron microscopy [(HRTEM) JEOL, JEM-4000EX]. The optical absorption spectra were measured using a Jasco V-500 UV/VIS spectrophotometer with a deuterium discharge tube (190–350 nm) and a tungsten–iodine lamp (330–900 nm). The magnetic properties of the nanorods were examined using superconducting quantum interference device magnetometer (Quantum Design, MPMS-7).

Figure 1(a) shows a typical SEM image of the $Zn_{1-x}Co_xO$ nanorods. A high density of well-aligned nanorods with a diameter in the range of 60–80 nm uniformly formed over the entire silicon substrate. EPMA taken from these nanorods in Fig. 1(a) shows that the atomic composition ratio of $(Zn_{1-x}Co_x):O$ is about 1:1. Diameter control of the well-aligned $Zn_{1-x}Co_xO$ nanorods in a certain range was

[a]Author to whom correspondence should be addressed; electronic mail: wujj@mail.ncku.edu.tw

 © 2004 American Institute of Physics
Downloaded 03 Oct 2008 to 140.116.208.41. Redistribution subject to AIP license or copyright; see http://apl.aip.org/apl/copyright.jsp

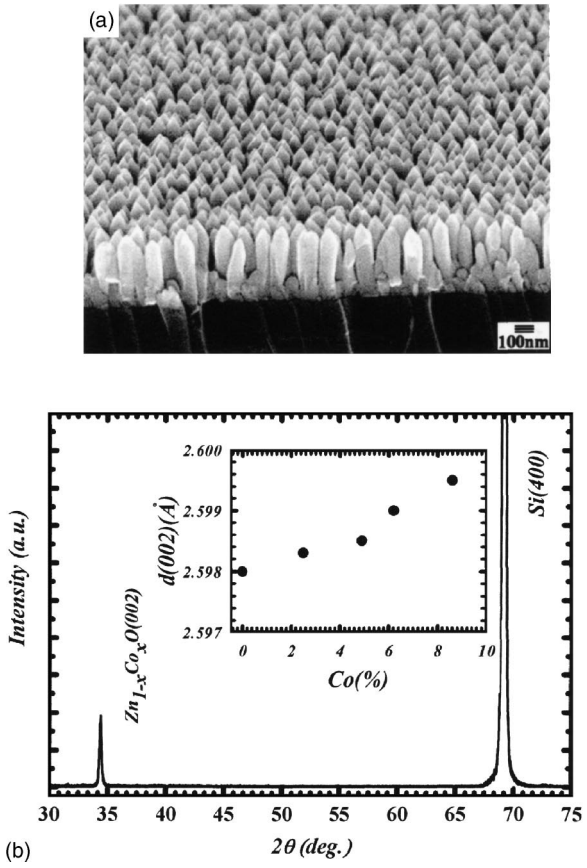

FIG. 1. (a) SEM image of the $Zn_{1-x}Co_xO$ nanorods. (b) XRD pattern of the $Zn_{1-x}Co_xO$ nanorods on a Si (100) substrate.

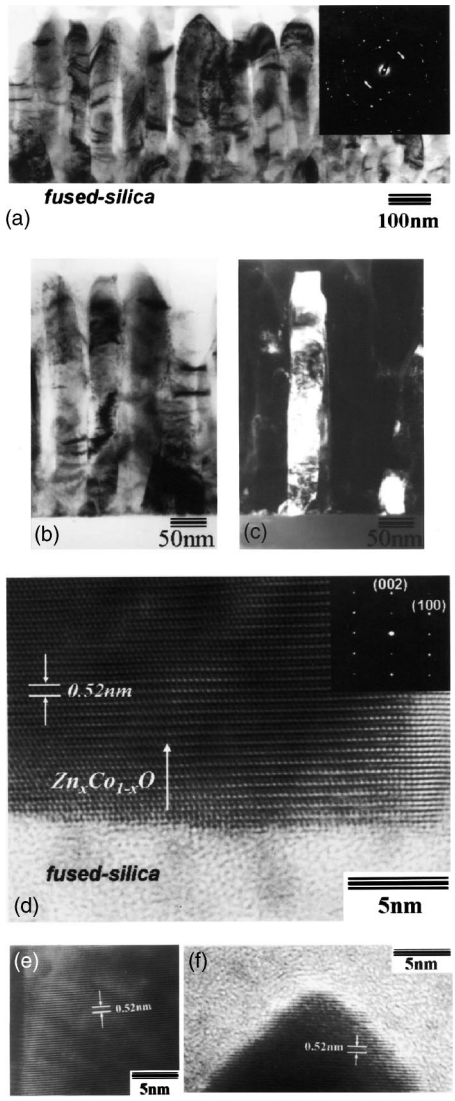

FIG. 2. TEM cross-sectional images of $Zn_{1-x}Co_xO$ ($x=0.037$) nanorods grown on fused silica substrates. (a) Low magnification image and SAD pattern (inset). (b) and (c) Typical bright-field and dark-field images of the $Zn_{1-x}Co_xO$ nanorods, respectively. (d)–(f) HRTEM image of the bottom, middle, and top regions of a single-crystalline $Zn_{1-x}Co_xO$ nanorod and the corresponding electron diffraction pattern (inset).

achieved by adjusting the growth conditions as in the case for ZnO nanorods.[12] Moreover, the atomic composition ratio of Zn:Co is adjustable by varying the vapor flux of cobalt acetylacetonate. The typical XRD pattern of the well-aligned $Zn_{1-x}Co_xO$ nanorods is illustrated in Fig. 1(b). In addition to Si (004) diffraction peak, the peak very close to (002) of the wurtzite structure of ZnO shows that the $Zn_{1-x}Co_xO$ nanorods possess the same structure as the ZnO nanorods and are preferentially oriented in the *c*-axis direction. The absence of the diffraction peaks of CoO and Co structures in the XRD pattern implies the Co incorporation within the ZnO nanorods by the means of substitution for Zn. The Co content dependence of the *c*-axis lattice constants [$d(002)$ values] is shown in the inset of Fig. 1(b). The $d(002)$ values increase with the Co concentrations within the $Zn_{1-x}Co_xO$ nanorods, implying that Co was systematically substituted for Zn in the nanorods.

Due to the detection limitation of the XRD measurement for the tiny nanocrystals, further structural characterization of the $Zn_{1-x}Co_xO$ nanorods was performed using transmission electron microscopy (TEM). It has been demonstrated that there is a SiO_x interfacial layer between the ZnO nanorods and Si substrates using this catalyst-free CVD method,[12] the $Zn_{1-x}Co_xO$ nanorods grown on the fused silica substrate for UV-visible absorption measurement were thus also employed to investigated the structural properties of the $Zn_{1-x}Co_xO$ nanorods. A cross-sectional TEM image of the $Zn_{1-x}Co_xO$ ($x=0.037$) nanorods on the fused silica substrate is shown in Fig. 2(a). It reveals that most of nanorods were grown in a direction perpendicular to the fused silica substrates. The selection area diffraction (SAD) pattern of the cross-sectional image shows a discrete ring pattern as illustrated in the inset of Fig. 2. All *d* spacings estimated from the SAD are close to those of the planes of the ZnO structure, confirming the XRD analyses that the CoO as well as Co phases are not observed in the nanorods. In addition, the discrete ring pattern indicates that the $Zn_{1-x}Co_xO$ nanorods are grown on the fused silica substrate randomly in the *a*-axis direction although they are preferentially oriented in the *c*-axis direction. Typical bright-field and dark-field images of the $Zn_{1-x}Co_xO$ nanorods are illustrated in Figs. 2(b) and 2(c), respectively. The dark-field image indicates that the nanorod possesses the single-crystalline structure. Figures 2(d)–2(f) show typical high-resolution TEM images of the bottom, middle, and top regions of an individual nanorod. There is no segregated cluster of impurity phase appearing throughout the nanorod.

Figure 3(a) shows the field dependences of magnetization ($M-H$ curves) of the 3.7%, 6.3%, and 8.7% Co-doped ZnO nanorods grown on the Si substrates measured at 300 K, in which the diamagnetic characteristic of the Si sub-

Downloaded 03 Oct 2008 to 140.116.208.41. Redistribution subject to AIP license or copyright; see http://apl.aip.org/apl/copyright.jsp

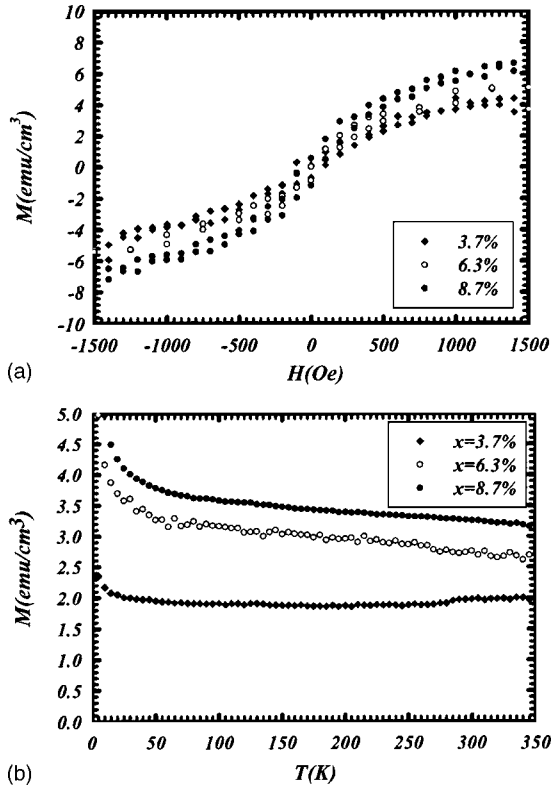

FIG. 3. (a) $M-H$ curves of the 3.7%, 6.3%, and 8.7% Co-doped ZnO nanorods grown on the Si substrate measured at 300 K. (b) Temperature dependence of magnetization for the $Zn_{1-x}Co_xO$ nanorods.

strates has been subtracted. They reveal that hysteresis curves with the coercive field (H_c) of 75 Oe are observed in the $Zn_{1-x}Co_xO$ nanorods, showing their ferromagnetic characteristic at 300 K. Moreover, the saturation magnetization (M_s) per unit volume of the $Zn_{1-x}Co_xO$ nanorods is increased with the Co concentration. The M_s of the $Zn_{1-x}Co_xO$ nanorods are estimated to be $0.22\pm0.01\ \mu_B$/Co site from the $M-H$ curves at 300 K. The temperature dependence of magnetization for the $Zn_{1-x}Co_xO$ nanorods is shown in Fig. 3(b). A magnetic field of 0.1 T was applied perpendicular to the long axes of the 3.7%, 6.3%, and 8.7% Co-doped ZnO nanorods. As shown in Fig. 3(b), the ferromagnetic properties are still maintained at a temperature of 350 K and T_C is thus estimated to be higher than 350 K.

The UV-visible absorption spectra of the $Zn_{1-x}Co_xO$ ($x=0.063$ and 0.091) and ZnO nanorods obtained at room temperature are shown in Fig. 4(a), indicating the transparence of the $Zn_{1-x}Co_xO$ nanorods in the visible region. Figure 4(b) presents the dependence of the absorption coefficients as a function of $h\nu(E)$ for the Co-doped ZnO nanorods as well as the pure ZnO nanorods. The intercepts defining the direct energy gaps[13] for the 6.3% and 9.1% Co-doped ZnO nanorods are 3.21 and 3.20 eV, respectively, which do not reveal pronounced difference from that of pure ZnO nanorods.

In summary, the formation of diluted magnetic semiconductor $Zn_{1-x}Co_xO$ nanorods using a simple CVD method has been demonstrated in this letter. A Curie temperature higher than 350 K was obtained in the well-aligned $Zn_{1-x}Co_xO$ nanorods. Structural analyses indicated that the nanorod pos-

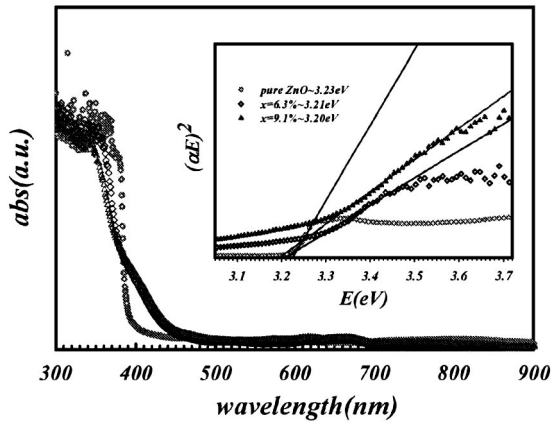

FIG. 4. (a) UV-visible absorption spectra and (b) dependence of the absorption coefficients as a function of $h\nu$ (E) of the $Zn_{1-x}Co_xO$ ($x=0.063$ and 0.091) and ZnO nanorods obtained at room temperature.

sesses the single-crystalline wurtzite structure. The transparence of the $Zn_{1-x}Co_xO$ nanorods in the visible region has been examined by UV-visible absorption. Combining the optical properties with room-temperature ferromagnetism, spintronic nanodevices would be made from the well-aligned ZnO-based DMSs possibly.

The authors would like to thank Professor Y. Chen and Dr. L. C. Chen for help with UV-visible absorption and high-resolution SEM measurements, respectively. The financial support of this work, by the National Science Council in Taiwan under Contract No. NSC-92-2214-E006-005, is gratefully acknowledged.

[1] H. Ohno, Science **281**, 951 (1998).
[2] S. J. Pearton, C. R. Abernathy, D. P. Norton, A. F. Hebard, Y. D. Park, L. A. Boatner, and J. D. Budai, Mater. Sci. Eng., R. **40**, 137 (2003).
[3] J. K. Furdyna, J. Appl. Phys. **64**, R29 (1988).
[4] T. Dietl, H. Ohno, F. Matsukura, J. Cibert, and D. Ferrand, Science **287**, 1019 (2000).
[5] Y. Chen, D. M. Bagnall, H. Koh, K. Park, K. Hiraga, Z. Zhu, and T. Yao, J. Appl. Phys. **84**, 3912 (1998).
[6] D. M. Bagnall, Y. F. Chen, Z. Zhu, T. Yao, S. Koyama, M. Y. Shen, and T. Goto, Appl. Phys. Lett. **70**, 2230 (1997); P. Zu, Z. K. Tang, G. K. L. Wong, M. Kawasaki, A. Ohtomo, H. Koinuma, and Y. Segawa, Solid State Commun. **103**, 459 (1997); H. Co, J. Y. Xu, E. W. Seelig, and R. P. H. Chang, Appl. Phys. Lett. **76**, 2997 (2000); M. H. Huang, S. Mao, H. Feick, H. Yan, Y. Wu, H. Kind, E. Weber, R. Russo, and P. Yang, Science **292**, 1897 (2001).
[7] K. Ueda, H. Tabata, and T. Kawai, *ibid.* **79**, 988 (2001); T. Fukumura, Z. Jin, M. Kawasaki, T. Shono, T. Hasegawa, S. Koshihara, and H. Koinuma, *ibid.* **78**, 958 (2001); J. H. Kim, H. Kim, D. Kim, Y. E. Ihm, and W. K. Choo, J. Appl. Phys. **92**, 6066 (2002).
[8] C. M. Lieber, Solid State Commun. **107**, 607 (1998); Y. Xia, P. Yang, Y. Sun, Y. Wu, B. Mayers, B. Gates, Y. Yin, F. Kim, and H. Yan, Adv. Mater. (Weinheim, Ger.) **15**, 353 (2003).
[9] S. W. Jung, W. I. Park, G. C. Yi, and M. Kim, Adv. Mater. (Weinheim, Ger.) **15**, 1358 (2003).
[10] K. Ip, R. M. Frazier, Y. W. Heo, D. P. Norton, C. R. Abernathy, S. J. Pearton, J. Kelly, R. Rairigh, A. F. Hebard, J. M. Zavada, and R. G. Wilson, J. Vac. Sci. Technol. B **21**, 1476 (2003).
[11] Y. Q. Chang, D. B. Wang, X. H. Luo, X. Y. Xu, X. H. Chen, L. Li, and C. P. Chen, Appl. Phys. Lett. **83**, 4020 (2003).
[12] J. J. Wu and S. C. Liu, Adv. Mater. (Weinheim, Ger.) **14**, 215 (2002); J. J. Wu, and S. C. Liu, J. Phys. Chem. B **106**, 9546 (2002).
[13] J. I. Pankove, *Optical Processes in Semiconductors* (Prentice–Hall, New Jersey, 1971), p.36.

Downloaded 03 Oct 2008 to 140.116.208.41. Redistribution subject to AIP license or copyright; see http://apl.aip.org/apl/copyright.jsp